Journal of Materials Chemistry B

ROYAL SOCIETY OF CHEMISTRY

PAPER

View Article Online
View Journal | View Issue

Cite this: J. Mater. Chem. B, 2023, 11, 3808

Phosphorene hydrogel conduits as "neurotrophin reservoirs" for promoting regeneration of peripheral nerves†

Tiankun Hui,[a] Chen Wang,[a] Liangmin Yu,[a] Chuanli Zhou*[b] and Meng Qiu *[a]

Received 19th February 2023,
Accepted 22nd March 2023

DOI: 10.1039/d3tb00340j

rsc.li/materials-b

Treatment of large gaps in peripheral nerves is a major clinical challenge. Artificial nerve guidance conduits (NGCs) have provided new opportunities for guiding nerve regeneration. In this study, multifunctional black phosphorus (BP) hydrogel NGCs loaded with neuregulin 1 (Nrg1) were fabricated to support peripheral-nerve regeneration: they exhibited good flexibility and nerve regeneration-related cell induction, promoted Schwann-cell proliferation and accelerated neuron-branch elongation. Nrg1 induced the proliferation and migration of Schwann cells, which had beneficial roles in promoting nerve regeneration. *In vivo* immunofluorescence studies revealed BP hydrogel NGCs loaded with Nrg1 promoted sciatic-nerve regeneration and axon remyelination. Our method has great potential for promoting treatment of peripheral-nerve injuries.

Introduction

Injury to peripheral nerves can lead to disability. Loss of neural control of organs leads to dysfunction of motor-sensory communication or even permanent disability.[1] The peripheral nervous system permits axon regeneration, but regenerative capacity is limited. End to-end tensionless repair of nerves results in suboptimal clinical results.[2–7] Autologous nerve grafting is the "gold standard" for large gaps in nerves, but universal application is severely hampered by donor-site morbidity and other side-effects.[8–10] Developments in tissue engineering and biomaterials have provided new opportunities for the construction of artificial "nerve guidance conduits" (NGCs) as alternatives to nerve autografts.[11] "Ideal" NGCs fulfill the criteria of biodegradability, mechanical softness, and tissue/cell inductive effect.[12–15] These properties bring high therapeutic efficacy without causing overt adverse effects.

Hydrogels are used widely as scaffolds in tissue engineering. Hydrogel-enriched NGCs provide a new opportunity to bridge large gaps in nerves and promote peripheral-nerve regeneration due to their biocompatibility, biodegradability and softness.[16,17] Among hydrogels, gelatin methacryloyl (GelMA) has been shown to be a promising scaffold.[18] However, its limited biomedical properties hamper its universal application in nerve regeneration. Thus, substantial efforts have been devoted to incorporate an inductive phase into the soft matrix to enhance the induction activity of NGCs. The emergence of two-dimensional materials (2DMs) has brought promising approaches to solve this problem. Black phosphorus (BP) is a 2DM with excellent electromechanical properties and biodegradability.[19] Due to these superior physicochemical properties, BP has attracted much attention in medical applications such as phototherapy and targeted drug delivery.[20–22] Notably, BP promotes osteogenesis and wound healing, which indicates that BP has tremendous potential in promoting tissue regeneration.[23–26] In particular, BP-based nerve conduits induce angiogenesis and neurogenesis under mild oxidative stress.[27] Besides, BP-incorporated hydrogels permit neural differentiation from mesenchymal stem cells.[28] These characteristics enable BP to be a versatile and promising therapeutic modality for promoting peripheral-nerve regeneration.

Neuregulin 1 (Nrg1) is part of the epidermal growth factor family. It is a multifunctional and versatile protein. Nrg1-regulated expansion and differentiation of Schwann cells has been regarded as compelling evidence for supporting nerve regeneration. Schwann cells, as glial cells in the peripheral nervous system, have pivotal roles in the development and maintenance of nerves but could also aid peripheral-nerve regeneration. By binding to receptors such as ErbB2/3, Nrg1 initiates an intracellular signaling pathway which provides a key signal to regulate the proliferation, migration and remyelination of Schwann cells.[29] Thus, potentiation of Schwann-cell behavior is one of the goals when constructing nerve NGCs.

In this study, we developed a BP hydrogel-based NGC by incorporating the neurotrophic factor Nrg1. BP incorporation

[a] Key Laboratory of Marine Chemistry Theory and Technology (Ocean University of China), Ministry of Education, Qingdao 266100, China
[b] Department of Spinal Surgery, The Affiliated Hospital of Qingdao University, No. 59 Haier Road, Qingdao, 266000, P. R. China. E-mail: zhoucl@qduhospital.cn

† Electronic supplementary information (ESI) available. See DOI: https://doi.org/10.1039/d3tb00340j

facilitated neurite growth, and this result was confirmed *in vitro* using a neuron cell line (PC12). In addition, under treatment with BP (500 μg mL^{-1}), proliferation of Schwann cells was observed. These results suggested that BP could be a highly desirable material for fabrication of NGCs. Furthermore, the porous structure and permeability of the hydrogel allowed controlled release of Nrg1. We demonstrated that Nrg1 (100 ng mL^{-1}) was optimal for promoting the proliferation of Schwann cells. This result was confirmed using the 5-ethynyl-2′-deoxyuridine (EdU) assay. In addition, Nrg1 promoted the migration of Schwann cells significantly. The effectiveness of BP hydrogel NGCs loaded with Nrg1 was evaluated further by *in vivo* animal experiments. In accordance with the *in vitro* result, BP hydrogel NGCs loaded with Nrg1 exhibited improved nerve regeneration. Our results provide a promising strategy for promoting peripheral-nerve regeneration.

Results and discussion

Design and fabrication of BP/GelMA/Nrg1 and characterization of mechanical properties

The transplantation process is shown as Fig. 1. BP hydrogel NGCs incorporated with Nrg1 were transplanted into the right sciatic nerve. The synthetic scheme for the hydrogel is shown as Fig. 2A. The gelatin solution was stirred until it became homogeneous. After dialysis, the solution was frozen and freeze-dried. After the GelMA pre-polymer solution had been irradiated under UV-light, the solution solidified and had a gelatinous texture, thereby indicating successful fabrication. Fig. 2B shows that BP had a good two-dimensional structure. The fabrication process of BP hydrogel NGCs loaded with Nrg1 is illustrated in Fig. 2C. GelMA, few-layered BP and Nrg1 composite hydrogels were mixed in an appropriate proportion. Conduits of diameter 1.2 mm and wall thickness of 0.5 mm were fabricated by perfusing this mixture into an annulus mold. After irradiation under UV-light, the mold was released along with NGCs. NGCs were implanted into rats with a large gap in nerves to assess their effectiveness.

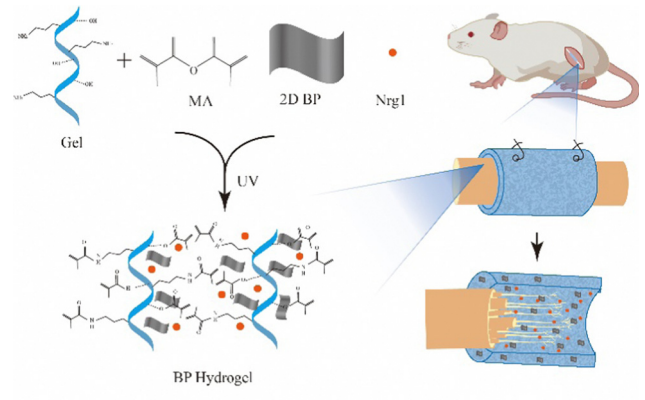

Fig. 1 BP hydrogel NGC incorporated with Nrg1 (schematic). BP hydrogel-based NGCs were soft and provided a "reservoir" for the loading and release of Nrg1. NGCs promoted nerve-dendrite elongation, as well as the proliferation and migration of Schwann cells to support nerve regeneration.

As shown in Fig. 3A, the NGCs had a length of 1.5 cm. The inner diameter and wall thickness were 1.2 mm and 0.5 mm, respectively. The mechanical property of NGCs was investigated to examine the feasibility of their use for transplantation *in vivo*. As shown in Fig. 3B, NGCs could bend from a small angle to nearly 180° without structural damage. This result indicated the good softness and mechanical property for *in vivo* transplantation. Next, the freeze-dried BP hydrogel NGCs loaded with Nrg1 were characterized by scanning electron microscopy (SEM): many pores were found within NGCs (Fig. S1, ESI†).

Biocompatibility and promoting effect on nerve regeneration of BP/GelMA/Nrg1 *in vitro*

Assessing the biocompatibility of materials was of pivotal importance for further *in vivo* application. Despite the universal employment of BP in biomedicine, its safety is controversial. Various exfoliation approaches or diverse architectures may be attributed to incomparable biocompatibilities. To evaluate the cytotoxicity of BP at different concentrations, the Cell Counting Kit (CCK)-8 assay was carried out. As shown in Fig. 4A, a low concentrations of BP promoted, whereas a high concentration impeded, the proliferation of Schwann cells. At 500 μg mL^{-1}, BP showed high efficiency for promoting the proliferation of Schwann cells. BP has been reported to enhance the neural differentiation of mesenchymal stem cells.[28] To investigate this ability, PC12 cells were induced into neuron-like shapes and treated with GelMA, BP or BP + Nrg1 for 7 days. After treatment, PC12 cells were stained with phalloidin to visualize and document their morphology. As depicted in Fig. 4B, compared with the hydrogel-treated group, BP hydrogel-treated cells showed an increased number of neuron dendrites and dendrite length. Furthermore, this phenomenon was intensified by addition of Nrg1. To further confirm these observations, the proportion of dendritic cells as well as the length and number of dendrites were calculated (Fig. 4C–E). The proportion of cells with branches was 33.37%, 57.22% and 82.98% in GelMA, BP and BP + Nrg1, groups, and the number of cell branches was 4.17, 5.16 and 6.0, respectively. This result suggested that BP treatment could facilitate formation of neuron branches (Fig. 4C and E). Furthermore, we measured the length of branches (19.86 μm, 31.66 μm and 59.05 μm in GelMA, BP and BP + Nrg1 groups, respectively). This result indicated that BP could promote elongation of neuron branches, and that Nrg1 further enhanced this phenomenon (Fig. 4D).

To evaluate the effects of Nrg1 on the proliferation of Schwann cells, we first undertook the CCK-8 assay (Fig. 5A). Clearly, Nrg1 was most effective in promoting cell proliferation at a concentration of 100 ng mL^{-1}. To gain more insights into how Nrg1 affected Schwann-cell proliferation, the EdU assay was carried out. Cells were seeded in a 96 well plate at an appropriate density. After cells had been treated with Nrg1 for 24 h, proliferated cells were labeled by the EdU assay kit. Many more green-labeled cells were found in the Nrg1-treated group, which indicated that Nrg1 addition was beneficial for Schwann-cell proliferation (Fig. 5B). The control group had 31.34%

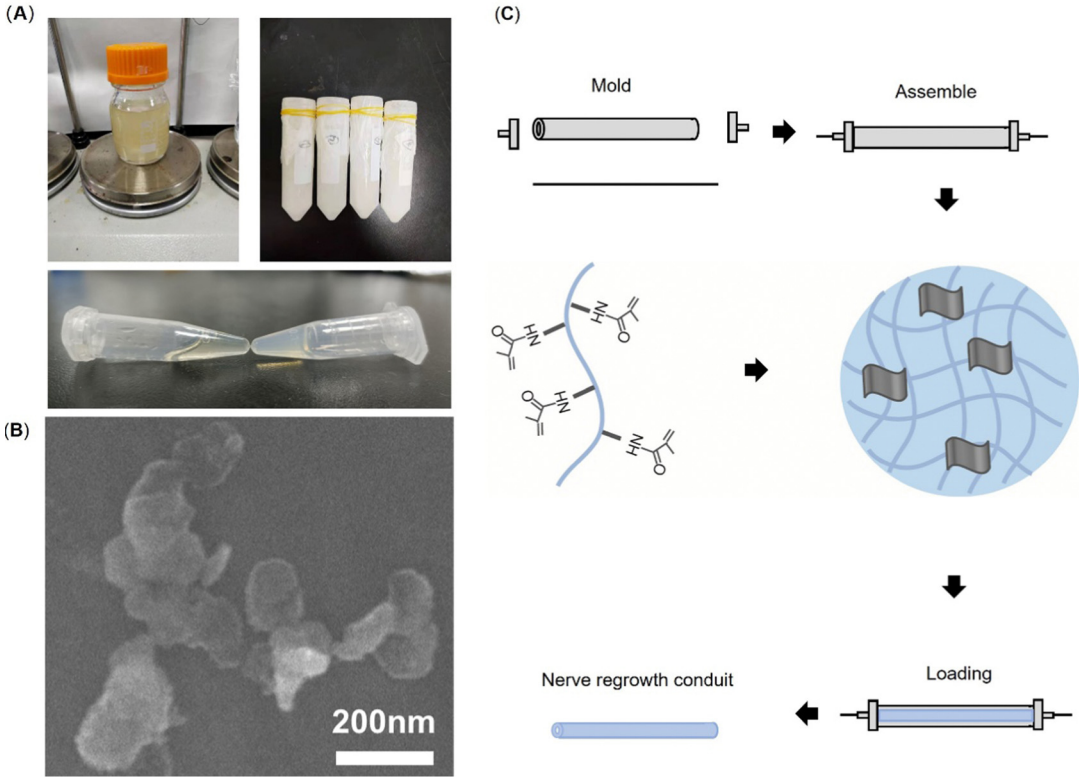

Fig. 2 GelMA synthesis and NGC fabrication. (A) Procedure for GelMA synthesis and image of solidified hydrogel. (B) SEM images of BP. (C) Annulus mold of diameter 2.2 mm and wall thickness 0.5 mm for NGCs fabrication.

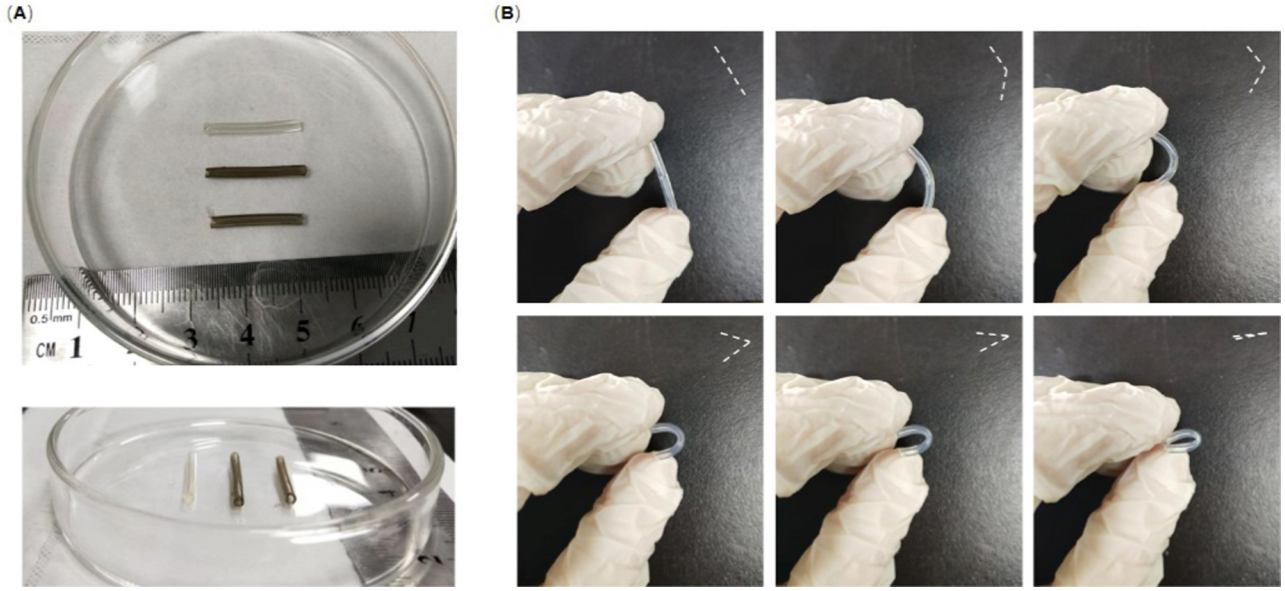

Fig. 3 Image and softness of NGCs. (A) NGCs photographs reveal the length to be 1.5 cm. (B) NGCs could be bent to 180° without suffering structural damage.

proliferated cells compared with 45.21% in Nrg1-treated cells (Fig. 5C). It was conceivable that, after nerve injury, the distal nerve end was affected.[2] Thus, improving the migration of Schwann cells could promote peripheral-nerve regeneration. To evaluate the effect of Nrg1 on cell migration, a Transwell™ experiment was carried out to simulate the migration of Schwann cells. The latter were seeded in the upper chamber and Nrg1 was dissolved in the lower chamber to induce cell

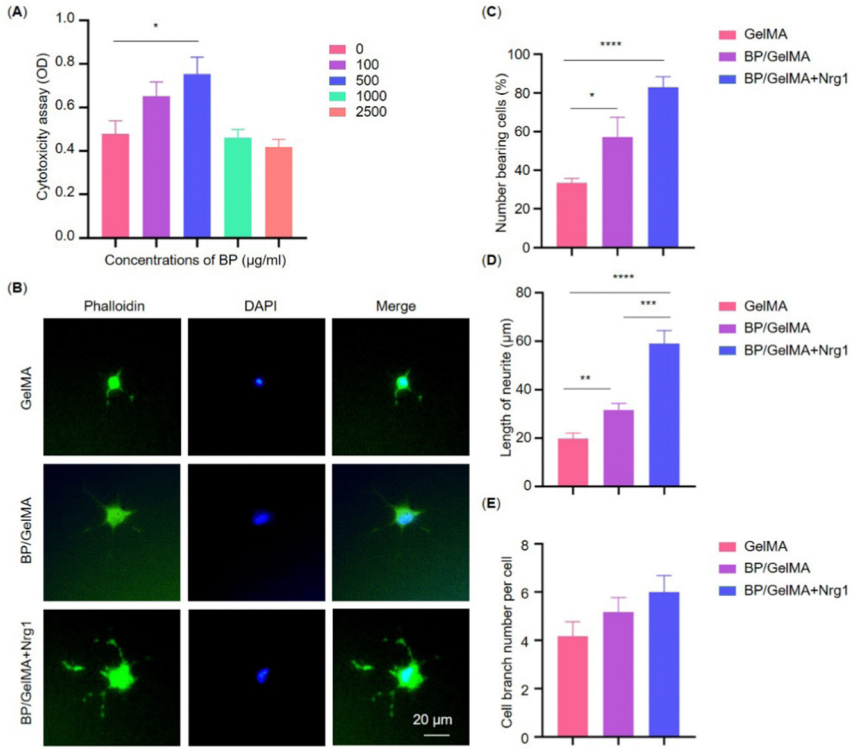

Fig. 4 BP promotes Schwann-cell proliferation and neuron differentiation. (A) The CCK-8 assay was employed to evaluate the effect of different concentrations of BP on Schwann-cell proliferation. (B) Neuron differentiation was evaluated by phalloidin staining. (C) Ratio of cells to dendrites. (D) Dendrite length. (E) Number of cell branches. *$P < 0.05$, **$P < 0.01$, ***$P < 0.001$, ****$P < 0.0001$.

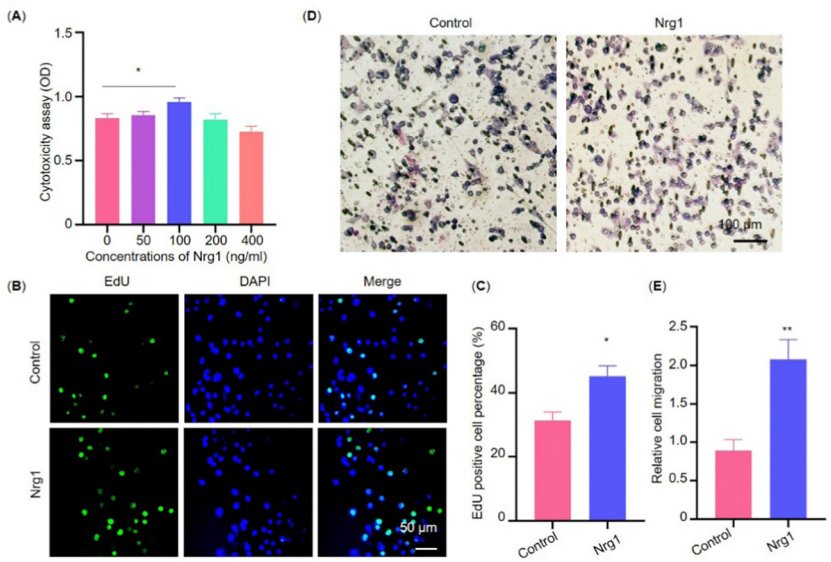

Fig. 5 Nrg1 promotes the proliferation and migration of Schwann cells. (A) The CCK-8 assay was employed to evaluate the effect of different concentrations of Nrg1 on Schwann-cell proliferation. (B) The EdU assay confirmed that Nrg1 could promote Schwann-cell proliferation. (C) The percentage of EdU-positive cells after Nrg1 treatment. (D) Nrg1 promoted Schwann-cell migration according to a Transwell™ experiment. (E) Effect of Nrg1 on relative migration of Schwann cells. *$P < 0.05$, **$P < 0.01$.

migration. After 24 h, approximately two-times more Schwann cells were found after Nrg1 treatment compared with those in the control group, which suggested that Nrg1 facilitated migration markedly (Fig. 5D and E). In accordance with a previous study, our results revealed Nrg1 to be a neurotrophic factor with potential for constructing NGCs. Together with the

superior properties of BP, we assumed that BP hydrogel-based NGCs incorporated with Nrg1 would augment therapeutic efficacy *in vivo*.

In vivo studies of NGC implantation

Encouraged by the potent promotion effect *in vitro*, we next investigated the effect of NGCs *in vivo*. Sprague–Dawley rats were anaesthetized and underwent nerve injury. NGCs (GelMA, BP/GelMA, BP/GelMA + Nrg1) of length 15 mm were implanted into the injury site to bridge nerve ends (Fig. 6A and B). Two months after surgery, rats were euthanized. The transplant, regenerated nerve allographs, tibialis anterior (TA) muscles, soleus muscles and extensor digitorum longus (EDL) muscles were harvested for further investigation. TA muscles, soleus muscles and EDL muscles were cross-sectioned. Hematoxylin and eosin (H&E) staining was carried out to evaluate the area of a single fiber in TA muscles. As shown in Fig. 6D, the muscle-fiber area in BP/GelMA + Nrg1 NGCs (1534 μm^2) transplanted groups was greater than that in BP/GelMA NGCs (1048 μm^2). A smaller muscle-fiber area was found in GelMA NGCs (403.7 μm^2) compared with that in other groups. These results were in accordance between the different muscle types we tested (Fig. S2A and S3A, ESI†).

Muscles were subjected to nerve innervation under normal conditions: when the muscle lost innervation, muscle atrophy occurred.[32,33] Hence, more muscle fibers were subjected to nerve innervation in BP + Nrg1 NGCs-transplanted groups. In other words, the regeneration of the sciatic nerve was accelerated. In addition, the formation of single muscle fibers of Schwann-cell cords between injured nerve bridge gaps is of vital importance for assisting nerve regeneration.[30,31] During this process, Schwann cells in proximal and distal nerve ends migrate to the injury site. They form Bngner bands and direct proximal nerve axons to regenerate.

In addition, the diameter of a single muscle fiber was evaluated. As shown in Fig. 6E, the result was in accordance with the muscle-area result. The diameter in GelMA-, BP/GelMA- and BP/GelMA + Nrg1 NGCs-treated groups was 22.37 μm, 35.92 μm and 43.6 μm, respectively. The diameter of each fiber was also evaluated in soleus muscles and EDL muscles: identical results were obtained (Fig. S2B and S3B, ESI†). In accordance with these results, a heavier muscle weight was found in the BP/GelMA + Nrg1 NGCs-treated group (Fig. 6F, Fig. S2C and S3C, ESI†).

To gain more information on nerve regeneration, we analyzed the neurofilament number after treatment. The sciatic nerve was isolated and cross-sectioned. Neurofilament antibody was used to label regenerated axons. Remarkably, more axons were found in BP/GelMA+ Nrg1 NGCs (neurofilament +/DAPI = 58.47%)-transplanted groups compared with GelMA (neurofilament +/DAPI = 30.59%) groups (Fig. 7A). A similar result for Schwann-cell number was obtained, which was in accordance with the result in Fig. 4A and 5A (Fig. 7C and D). This effect occurred along axons: remyelination.[34]

Remyelination has a pivotal role in the recovery of nerve function.[35] If nerve regeneration occurs, Schwann cells could send signals to stimulate myelin reproduction, thereby ensuring normal conduction of electrical signals. BP/GelMA + Nrg1 NGCs accelerated the proliferation of Schwann cells but whether remyelination was reinforced as a consequence was not clear. To test our hypothesis, nerves were fixed with

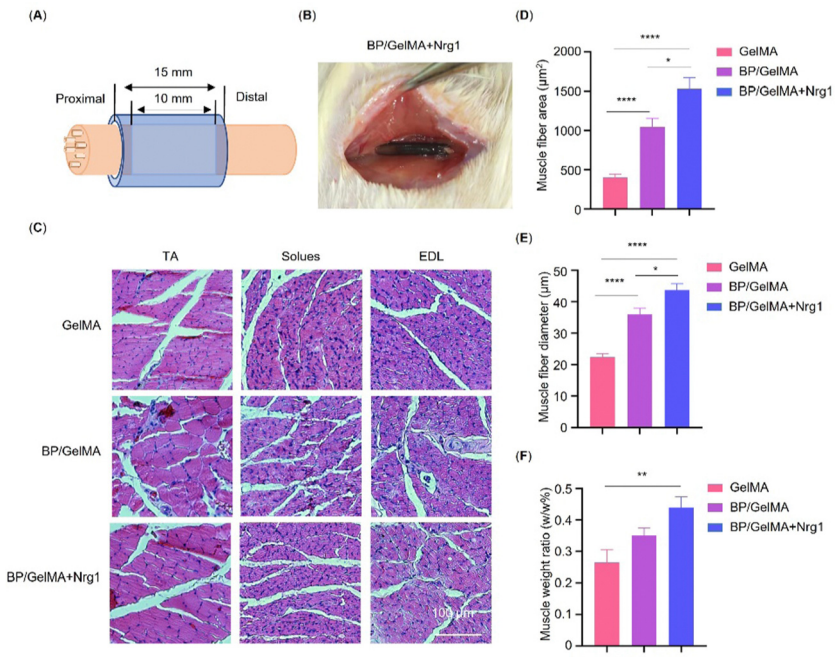

Fig. 6 *In vivo* histology of regenerated muscles 2 months post-operation. (A) Transplanted NGCs (schematic). (B) Photograph of transplanted BP/GelMA + Nrg1 NGCs *in vivo*. (C) H&E staining of slices of the TA muscle, soleus muscle and EDL muscle in each group 2 months post-operation. (D–F) Fiber area, diameter and weight ratio in the TA muscle. *$P < 0.05$, **$P < 0.01$, ****$P < 0.0001$.

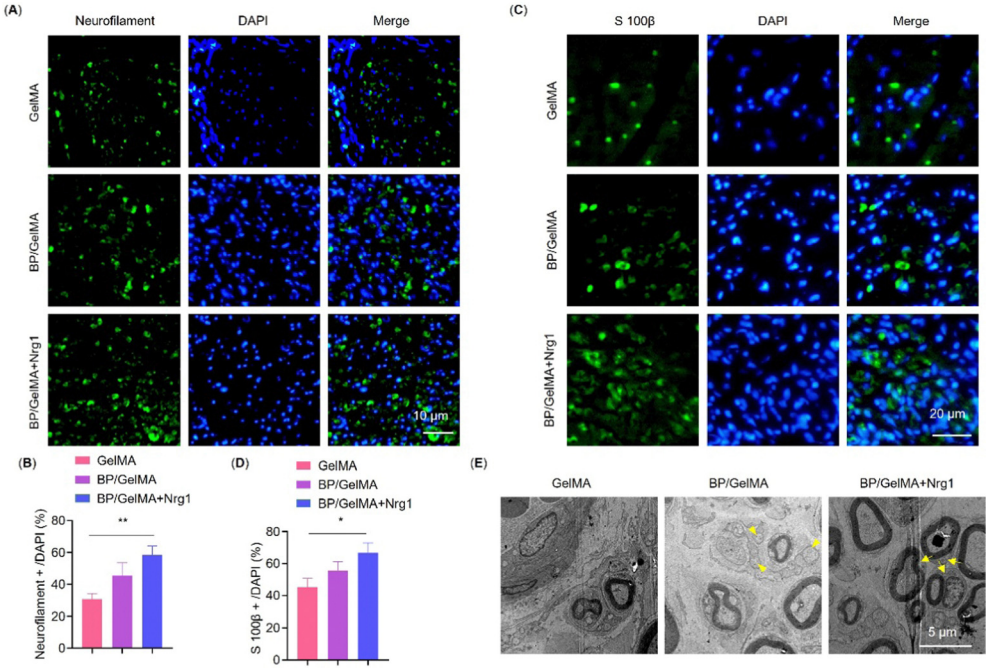

Fig. 7 Histology of the regenerated sciatic nerve 2 months post-operation. (A) Immunofluorescence staining of regenerated axons. (B) Quantification of neurofilaments. (C) Immunofluorescence staining of Schwann cells. (D) Quantification of Schwann cells. (E) TEM images of axon remyelination. The arrowhead indicates axons lacking myelin. The arrow indicates Schwann cells attached to myelinated axons. $*P < 0.05$, $**P < 0.01$.

glutaraldehyde and cross-sectioned. The TEM image revealed more myelinated axons in the BP/GelMA + Nrg1 NGCs-treated group compared with that in other groups, which indicated accelerated nerve regeneration and remyelination in the BP/GelMA + Nrg1 NGCs-treated group (Fig. 7E). In that group, Schwann cells were attached to myelinated axons. In the BP/GelMA NGCs-treated group, some axons with no myelin were found. In the GelMA NGCs-treated group, only a few axons were remyelinated few axons were found. In addition, the diameter of axons was calculated: it was 1.135 μm, 1.987 μm and 2.653 μm in GelMA, BP/GelMA and BP/GelMA + Nrg1 NGCs transplantation groups, respectively (Fig. S4A, ESI†). Furthermore, thicker myelin was found in the BP/GelMA + Nrg1 NGCs transplantation group compared with that in other groups (Fig. S4B, ESI†).

Taken together, our results suggest NGCs could promote peripheral-nerve regeneration.

Conclusions

We created BP hydrogel NGCs that could serve as a Nrg1 reservoir for guiding peripheral-nerve regeneration. These flexible NGCs could endure with bending to 180°. To assess the effect of BP on nerve regeneration, different concentrations of BP were used to evaluate cell viability. We found that BP at 500 μg mL^{-1} could induce Schwann-cell proliferation while higher concentrations were cytotoxic. BP also influenced the development and elongation of neuron branches. In addition, we determined the effect of Nrg1 on the proliferation and migration of Schwann cells. We first investigated the behavior of Schwann cells under different concentrations of Nrg1. Under treatment of Nrg1 at 100 ng mL^{-1}, proliferation of Schwann cells was prominent. This result was confirmed by the EdU assay. Furthermore, migration of Schwann cells was increased significantly by Nrg1 addition. *In vivo* studies demonstrated that, BP/GelMA + Nrg1 NGCs improved muscle reinnervation. Greater numbers of neurofilaments and Schwann cells were found compared with those in other groups. The number of remyelinated axons was enhanced in BP/GelMA + Nrg1 NGCs-transplanted groups. Our results suggest that BP/GelMA + Nrg1 NGCs are good candidates for clinical development.

Experimental procedure

Materials

Bulk BP was purchased from a local commercial supplier (Smart-Elements). NMP and other synthesis-related reagents were purchased from Aladdin Reagents (Beijing, China) unless stated. otherwise Dulbecco's phosphate-buffered saline (DPBS), Dulbecco's modified Eagle's medium (DMEM), fetal bovine serum (FBS), and horse serum (HS) were obtained from Gibco (Rockville, MD, USA). Primary antibodies were purchased from Abcam (Cambridge, UK). AlexaFluor-488 secondary antibody was from Invitrogen (Carlsbad, CA, USA). Hydromount was purchased from National Diagnostics (Kolkata, India).

Synthesis of GelMA

Gelatin (10%) was dissolved in prewarmed DPBS (60 °C) and added dropwise into methacrylic anhydride (0.8 mL g^{-1}) solution with stirring. After stirring for 2 h, 40 mL of DPBS (40 °C) was added to the solution. The solution was transferred into a pretreated dialysis bag. Dialysis was carried out at 40 °C

with water change once a day for 1 week. After passing through a 0.2 μm filter, the solution was transferred into a 50 mL tube and freeze-dried for subsequent experiments.

Synthesis of GelMA hydrogel NGC

GelMA (20% w/v) and designated BP were dissolved in DPBS with a photo-initiator (0.05% w/v). The mixed solution was added to a glass tube (inner diameter = 2.2 mm) with a rod (diameter = 1.2 mm) fixed into the center. After exposure to UV light for 5 min, the mixture was crosslinked into GelMA-BP hydrogel and demolded.

Characterization of various hydrogel NGCs

To analyze NGC morphology, BP + Nrg1 NGC was freeze-dried and cut into small sections for SEM.

CCK-8 assay

To evaluate the effect of BP and Nrg1 upon cells, extracts of GelMA-BP hydrogel and GelMA-Nrg1 hydrogel were abstracted. About 80 μL of GelMA-BP hydrogel or GelMA-Nrg1 hydrogel solutions with different concentrations of BP and Nrg1 were added to 96 well plates. After crosslinking under exposure to UV light, RSC96 culture medium (120 μL) was added and incubation in a cell incubator undertaken overnight. RSC96 cells were incubated with 100 μL of extracts for an appropriate time and detected by a microplate reader (Multiskan GO; Thermo Fisher Scientific, Waltham, MA, USA).

EdU assay

Cells were pretreated with GelMA-Nrg1 hydrogel extracts for 24 h. Then, cells were treated with the same volume of mixed culture medium and 2× EdU working solution for an appropriate time. After incubation with a click reaction solution for 20–30 min at room temperature, the medium was discarded and cells were washed thrice with DBPS. Then, cells were stained with DAPI and observed under a fluorescence microscope (IX73; Olympus, Tokyo, Japan).

Transwell assay

A Transwell apparatus (Corning, Corning, NY, USA) was used to assay Nrg1-induced cell migration. First, cells were suspended in 500 μL of serum-free medium and added to a 24 well plate in the upper chamber. Second, the culture medium with Nrg1 was added to the lower chamber. After incubation at 37 °C for 24 h, cells in the upper membrane were removed and the chamber was fixed in 4% paraformaldehyde. Finally, cells migrating to the other side were stained with crystal violet and images under a microscope (IX73; Olympus) taken.

In vivo study

Experiments conformed strictly to guidelines for animal care in laboratories. All animals received humane care and all procedures were approved (20220116SD1820220331002) by the Experimental Animal Welfare Ethics Committee of Qingdao University. All animals were housed in a pathogen-free experimental animal room at a suitable temperature and day/night cycle. Eighteen male Sprague–Dawley rats (~200 g) were divided into three groups. After 1 week, rats were anesthetized. Their right-thigh fur was shaved and sterilized with 75% alcohol. After making a skin incision, the sciatic nerve was exposed. A ~1 cm segment was excised and replaced with hydrogel NGCs. The nerve end, NGCs and skin were sutured. Mice were placed on a warm rubber pad until they regained consciousness.

H&E staining

Fresh-frozen muscle tissues were made into cryosections. Then, the tissue slices were washed thrice with PBS to remove residual mounting medium and incubated in hematoxylin for 15 min. After rinsing in running deionized water for 5 min, the slices were embedded in eosin for 3 min. Then, the slices were dehydrated sequentially with a graded series of ethanol solutions (75, 95 and 100%) for 3 min each time, and incubated with xylene for 20 min. Finally, the slices were mounted with cytoseal and images were captured under a microscope (IX73; Olympus).

Immunofluorescence staining

Nerve segments were cross-sectioned into (thickness = 20 μm) and fixed in 4% PFA for 20 min. After washing thrice with PBS, the slices were incubated in blocking buffer for 2 h at room temperature. The primary antibody was diluted in blocking buffer to an appropriate concentration. Then, the slices were incubated with the primary antibody at 4 °C overnight. After washing thrice, the slices were incubated with secondary antibody for 2 h at room temperature. Finally, samples were washed and mounted with Hydromount. After samples had been air-dried, images were captured under a microscope (IX73; Olympus).

Author contributions

T. H. and M. Q. designed the study and supervised the project. T. H. performed the experiments. T. H. and C. W. wrote the manuscript. M. Q., L. Y. and C. Z. reviewed and edited the manuscript.

Conflicts of interest

The authors declare no conflict of interest.

Acknowledgements

This work was supported by the National Natural Science Foundation of China (U1803128), Taishan Scholar Project (tsqn201909054), Natural Science Foundation of Shandong Province (ZR202110290057), and Fundamental Research Funds for the Central Universities to M. Q.

References

1 S. Zhu, J. Ge, Y. Wang, F. Qi, T. Maa, M. Wang, Y. Yang, Z. Liu, J. Huang and Z. Luo, *Biomaterials*, 2014, **35**, 1450–1461.
2 Q. Min, D. B. Parkinson and X.-P. Dun, *Glia*, 2020, **69**, 235–254.
3 M. MahariD and V. Cavalli, *Nat. Rev. Neurosci.*, 2018, **6**, 323–337.
4 Y. Gao, Y.-l Wang, D. Kong, B. Qu, X.-j Su, H. Li and H.-Y. Pi, *Neural Regen. Res.*, 2015, **10**, 1003–1008.
5 W. Z. Ray and S. E. Mackinnon, *Exp. Neurol.*, 2010, **1**, 77–85.
6 L. B. Dahlin, *Scand. J. Surg.*, 2008, **4**, 310–316.
7 K. Allbright, J. Bliley, E. Havis, D.-Y. Kim, G. A. Dibernardo, D. Grybowski, M. Waldner, I. B. James, W. N. Sivak, J. P. Rubin and K. G. Marra, *Muscle Nerve*, 2018, **2**, 251–260.
8 O. Alluin, C. Wittmann, T. Marqueste, J.-F. Chabas, S. Garcia, M.-N. Lavaut, D. Guinard, F. Feron and P. Decherchi, *Biomaterials*, 2009, **30**, 363–373.
9 V. Carriel, J. Garrido-Gómez, P. Hernández-Cortés, I. Garzón, S. García-García, J. Sáez-Moreno, M. Sánchez-Quevedo1, A. Campos and M. Alaminos, *J. Neural Eng.*, 2013, **2**, 026022.
10 F. Xiang, D. Wei, Y. Yang, H. Chi, K. Yang and Y. Sun, *Neurosci. Lett.*, 2017, **638**, 114–120.
11 W. A. Lackington, A. J. Ryan and F. J. O'Brien, *ACS Biomater. Sci. Eng.*, 2017, **3**, 1221–1235.
12 L. Wang, C. Lu, S. Yang, P. Sun, Y. Wang, Y. Guan, S. Liu, D. Cheng, H. Meng, Q. Wang, J. He, H. Hou, H. Li, W. Lu, Y. Zhao, J. Wang, Y. Zhu, Y. Li, D. Luo, T. Li, H. Chen, S. Wang, X. Sheng, W. Xiong, X. Wang, J. Peng and L. Yin, *Sci. Adv.*, 2020, **50**, eabc6686.
13 H. Xu, J. M. Holzwarth, Y. Yan, P. Xu, H. Zheng, Y. Yin, S. Li and P. X. Ma, *Biomaterials*, 2014, **35**, 225–235.
14 J. Park, J. Jeon, B. Kim, M. S. Lee, S. Park, J. Lim, J. Yi, H. Lee, H. S. Yang and J. Y. Lee, *Adv. Funct. Mater.*, 2020, **30**, 2003759.
15 J. Xie, M. R. MacEwan, W. Liu, N. Jesuraj, X. Li, D. Hunter and Y. Xia, *ACS Appl. Mater. Interfaces*, 2014, **6**, 9472–9480.
16 Q. Huang, Y. Cai, X. Zhang, J. Liu, Z. Liu, B. Li, H. Wong, F. Xu, L. Sheng, D. Sun, J. Qin, Z. Luo and X. Lu, *ACS Appl. Mater. Interfaces*, 2021, **13**, 112–122.
17 X. Liu, A. L. Miller, S. Park, B. E. Waletzki, Z. Zhou, A. Terzic and L. Lu, *ACS Appl. Mater. Interfaces*, 2017, **9**, 14677–14690.
18 Y. Hu, Y. Wu, Z. Gou, J. Tao, J. Zhang, Q. Liu, T. Kang1, S. Jiang, S. Huang, J. He, S. Chen, Y. Du and M. Gou, *Sci. Rep.*, 2016, **6**, 32184.
19 H. Wang and X.-F. Yu, *Small*, 2017, **14**, 1702830.
20 M. Qiu, D. Wang, W. Liang, L. Liu, Y. Zhang, X. Chen, D. K. Sang, C. Xing, Z. Li, B. Dong, F. Xing, D. Fan, S. Bao, H. Zhang and Y. Cao, *Proc. Natl. Acad. Sci. U. S. A.*, 2018, **115**, 501–506.
21 W. Chen, J. Ouyang, H. Liu, M. Chen, K. Zeng, J. Sheng, Z. Liu, Y. Han, L. Wang, J. Li, L. Deng, Y. N. Liu and S. Guo, *Adv. Mater.*, 2017, **29**, 201603864.
22 X. Zeng, M. Luo, G. Liu, X. Wang, W. Tao, Y. Lin, X. Ji, L. Nie and L. Mei, *Adv. Sci.*, 2018, **5**, 510–518.
23 B. Yang, J. Yin, Y. Chen, S. Pan, H. Yao, Y. Gao and J. Shi, *Adv. Mater.*, 2018, **10**, 201705611.
24 L. Cheng, Z. Cai, J. Zhao, F. Wang, M. Lua, L. Deng and W. Cui, *Bioact. Mater.*, 2020, **4**, 1026–1043.
25 Y. Wang, X. Hu, L. Zhang, C. Zhu, J. Wang, Y. Li, Y. Wang, C. Wang, Y. Zhang and Q. Yuan, *Nat. Commun.*, 2019, **10**, 2829.
26 C. Mao, Y. Xiang, X. Liu, Z. Cui, X. Yang, Z. Li, S. Zhu, Y. Zheng, K. W. K. Yeung and S. Wu, *ACS Nano.*, 2018, **12**, 1747–1759.
27 Y. Qian, W. E. Yuan, Y. Cheng, Y. Yang, X. Qu and C. Fan, *Nano Lett.*, 2019, **19**, 8990–9001.
28 C. Xu, Y. Xu, M. Yang, Y. Chang, A. Nie, Z. Liu, J. Wang and Z. Luo, *Adv. Funct. Mater.*, 2020, **30**, 2000177.
29 Y. K. Shin, S. Y. Jang, S. H. Yun, Y. Y. Choi, B.-A. Yoon, Y. R. Jo, S. Y. Park, M. G. Pak, J. I. Park and H. T. Park, *Glia*, 2017, **65**, 1794–1808.
30 P. Arthur-Farraj and K. R. Jessen, *Glia*, 2019, **67**, 421–437.
31 X. N. S. Bolívar and E. Udina, *Cells*, 2020, **9**, 2131.
32 S. Afzal, H. T. Langer, S. Kempa and S. Spuler, *Sci. Rep.*, 2020, **10**, 1908.
33 P. Xue, X. Yang, H. Chen, M. Yuan, Y. Kang, D. Duscher, H. Machens and Z. Chen, *Theranostics*, 2020, **10**, 1415–1432.
34 A. R. R. K. Susuki, Y. Ogawa, M. C. Stankewich, E. Peles, W. S. Talbot and M. N. Rasband, *Proc. Natl. Acad. Sci. U. S. A.*, 2011, **108**, 8009–8014.
35 R. Stassart, R. Fledrich, V. Velanac, B. Brinkmann, M. Schwab, D. Meijer, M. Sereda and K. Nave, *Nat. Neurosci.*, 2013, **16**, 48–54.